Video Article

FM Dye Cycling at the Synapse: Comparing High Potassium Depolarization, Electrical and Channelrhodopsin Stimulation

Danielle L. Kopke[1], Kendal Broadie[2]

[1]Department of Biological Sciences, Vanderbilt University

[2]Departments of Biological Sciences, Pharmacology, Cell and Developmental Biology, Kennedy Center for Research on Human Development, Vanderbilt University and Medical Center

Correspondence to: Kendal Broadie at kendal.broadie@vanderbilt.edu

URL: https://www.jove.com/video/57765
DOI: doi:10.3791/57765

Keywords: Neuroscience, Issue 135, *Drosophila*, neuromuscular junction, FM1-43, electrophysiology, photoconversion, transmission electron microscopy

Date Published: 5/24/2018

Citation: Kopke, D.L., Broadie, K. FM Dye Cycling at the Synapse: Comparing High Potassium Depolarization, Electrical and Channelrhodopsin Stimulation. *J. Vis. Exp.* (135), e57765, doi:10.3791/57765 (2018).

Abstract

FM dyes are used to study the synaptic vesicle (SV) cycle. These amphipathic probes have a hydrophilic head and hydrophobic tail, making them water-soluble with the ability to reversibly enter and exit membrane lipid bilayers. These styryl dyes are relatively non-fluorescent in aqueous medium, but insertion into the outer leaflet of the plasma membrane causes a >40X increase in fluorescence. In neuronal synapses, FM dyes are internalized during SV endocytosis, trafficked both within and between SV pools, and released with SV exocytosis, providing a powerful tool to visualize presynaptic stages of neurotransmission. A primary genetic model of glutamatergic synapse development and function is the *Drosophila* neuromuscular junction (NMJ), where FM dye imaging has been used extensively to quantify SV dynamics in a wide range of mutant conditions. The NMJ synaptic terminal is easily accessible, with a beautiful array of large synaptic boutons ideal for imaging applications. Here, we compare and contrast the three ways to stimulate the *Drosophila* NMJ to drive activity-dependent FM1-43 dye uptake/release: 1) bath application of high [K^+] to depolarize neuromuscular tissues, 2) suction electrode motor nerve stimulation to depolarize the presynaptic nerve terminal, and 3) targeted transgenic expression of channelrhodopsin variants for light-stimulated, spatial control of depolarization. Each of these methods has benefits and disadvantages for the study of genetic mutation effects on the SV cycle at the *Drosophila* NMJ. We will discuss these advantages and disadvantages to assist the selection of the stimulation approach, together with the methodologies specific to each strategy. In addition to fluorescent imaging, FM dyes can be photoconverted to electron-dense signals visualized using transmission electron microscopy (TEM) to study SV cycle mechanisms at an ultrastructural level. We provide the comparisons of confocal and electron microscopy imaging from the different methods of *Drosophila* NMJ stimulation, to help guide the selection of future experimental paradigms.

Video Link

The video component of this article can be found at https://www.jove.com/video/57765/

Introduction

The beautifully-characterized *Drosophila* larval neuromuscular junction (NMJ) glutamatergic synapse model has been used to study synapse formation and function with a vast spectrum of genetic perturbations[1]. The motor neuron terminal consists of multiple axon branches, each with many enlarged synaptic boutons. These capacious varicosities (up to 5 µm in diameter) contain all of the neurotransmission machinery, including uniform glutamatergic synaptic vesicles (SVs; ~40 nm in diameter) in cytosolic reserve and readily-releasable pools[2]. These vesicles dock at the presynaptic plasma membrane fusion site active zones (AZs), where exocytosis mediates the glutamate neurotransmitter release for *trans*-synaptic communication. Subsequently, the SVs are retrieved from the plasma membrane via kiss-and-run recycling or clathrin-mediated endocytosis (CME) for repeated exo/endocytosis cycles. The *Drosophila* NMJ is easily accessible and well-suited for both isolating and characterizing SV cycle mutants. Using forward genetic screens, novel mutations have led to the identification of new genes critical for the SV cycle[3]. Moreover, reverse genetic approaches starting with already known genes have led to the elucidation of new SV cycle mechanisms through the careful description of mutant cycling phenotypes[4]. The *Drosophila* NMJ is nearly ideal as an experimental synaptic preparation for dissecting SV endocytosis and exocytosis mechanisms via methods to optically track vesicle cycling during neurotransmission.

A range of fluorescent markers allow visual tracking of vesicles during cycling dynamics, but the most versatile are FM dye analogs which is first synthesized by Mao, F., *et al.*[5]. Structurally, FM dyes contain a hydrophilic head and a lipophilic tail connected through an aromatic ring, with a central region conferring spectral properties. These styryl dyes partition reversibly in membranes, do not 'flip-flop' between membrane leaflets and so are never free in the cytosol, and are far more fluorescent in membranes than water[5]. Reversible insertion into a lipid bilayer causes a 40-fold increase in fluorescence[6]. At neuronal synapses, classic FM dye labeling experiments consist of bathing the synaptic preparation with the dye during depolarizing stimulation to load dye via SV endocytosis. External dye is then washed away and the SV cycle is arrested in a calcium-free ringer solution to image loaded synapses[7]. A second round of stimulation in a dye-free bath triggers FM release through exocytosis, a process that can be followed by measuring the fluorescence intensity decrease. SV populations from a single vesicle to pools containing hundreds of vesicles can be quantitatively monitored[6,7]. FM dyes have been used to dissect activity-dependent mobilization of functionally

distinct SV pools, and to compare kiss-and-run vs. CME cycling[8,9]. The method has been modified to separately assay evoked, spontaneous and miniature synaptic cycle activities (with highly sensitive equipment to detect very small fluorescence changes and reduce photobleaching)[10]. Assays can be extended to the ultrastructural level by photoconverting the fluorescent FM signal into an electron-dense label for transmission electron microscopy[11,12,13,14].

Historically, bathing synaptic preparations in a high concentration of potassium (hereafter referred to as "high [K^+]") has been the method of choice for depolarizing stimulation to induce SV cycling; ranging from the frog cholinergic NMJ[5], to cultured rodent brain hippocampal neurons[15], to the *Drosophila* glutamatergic NMJ model[16,17]. This high [K^+] approach is simple, requires no specialized equipment, and is therefore accessible to most labs, but has limitations for both application and data interpretation. A much more physiologically appropriate method is to use suction electrode electrical stimulation of the nerve[4,5,12]. This approach drives action potential propagation for direct stimulation of the presynaptic nerve terminal, and results can be directly compared to electrophysiological assays of neurotransmission function[13,14,15], but requires specialized equipment and is technically much more challenging. With the advent of optogenetics, the use of channelrhodopsin neuronal stimulation has additional advantages, including tight spatiotemporal control of channel expression using the binary Gal4/UAS system[20]. This approach is technically much easier than suction electrode stimulation and requires nothing more than a very cheap LED light source. Here, we employ imaging of FM1-43 (*N*-(3-triethylammoniumpropyl)-4-(4-(dibutylamino)styryl) pyridinium dibromide) to both compare and contrast these three different stimulation methods at the *Drosophila* NMJ: simple high [K^+], challenging electrical and new channelrhodopsin approaches.

Protocol

1. Larval Glue Dissection

1. Thoroughly mix 10 parts of silicone elastomer base with 1 part of silicone elastomer curing agent from the elastomer kit (**Table of Materials**).
2. Coat 22 x 22 mm glass coverslips with the elastomer and cure on a hot plate at 75 ˚C for several hours (until no longer sticky to the touch).
3. Place a single elastomer-coated glass coverslip into the custom-made plexi glass dissection chamber (**Figure 1**, bottom) in preparation for the larval dissection.
4. Prepare the glue pipettes from borosilicate glass capillary using a standard microelectrode puller to obtain the desired taper and tip size.
5. Gently break off the micropipette tip, and to the other end, attach 2 ft of flexible plastic tube (1/32" interior diameter, ID; 3/32" outside diameter, OD; 1/32" wall; **Table of Materials**) with mouth fitting (P2 pipette tip).
6. Fill a small container (0.6 mL Eppendorf tube cap) with a small volume (~20 µL) of glue (**Table of Materials**) in preparation for the larval dissection.
7. Fill the chamber with saline (in mM): 128 NaCl, 2 KCl, 4 $MgCl_2$, 1 $CaCl_2$, 70 sucrose, and 5 2-[4-(2-hydroxyethyl)piperazin-1-yl]ethanesulfonic acid (HEPES) pH 7.2.
8. Add anti-horse radish peroxidase (HRP) antibody conjugated to Alexa Fluor 647 (anti-HRP:647; dilute 1:10 from a 1 mg/mL stock) for labeling the NMJ presynaptic terminal during dissection[21,22].
9. Using a fine paintbrush (size 2), remove a wandering third instar from the food vial and place onto the elastomer-coated cover glass.
10. Fill the glass micropipette tip with a small volume of glue using negative air pressure generated by mouth with attachment (step 1.5).
11. Position larva dorsal side up with forceps and glue the head to the elastomer-coated coverslip with a small drop of glue using positive air pressure by mouth.
12. Repeat this procedure with the posterior end of the larva, making sure that the animal is stretched taut between the two glue attachments.
13. Using scissors (blades 3 mm; **Table of Materials**), make a horizontal cut (~1 mm) at posterior and a vertical cut all along the dorsal midline.
14. Using fine forceps (#5, **Table of Materials**), gently remove dorsal trachea, gut, fat body and other internal organs covering the musculature.
15. Repeat the gluing procedure for the four body wall flaps, making sure to gently stretch the body wall both horizontally and vertically.
16. Lift the ventral nerve cord (VNC) using forceps, carefully cut the motor nerves with the scissors, and then completely remove the VNC.
17. Replace the dissection saline with Ca^{2+}-free saline (same as the above dissection saline without the $CaCl_2$) to stop SV cycling.

2. Option 1: High [K^+] FM Dye Loading

1. From a FM1-43 stock solution (4 mM), add 1 µL to 1 mL of 90 mM KCl solution (high [K^+] in dissection saline) for a final concentration of 4 µM.
2. Using a pipette, replace the Ca^{2+}-free saline in the imaging chamber with the high [K^+] FM dye solution to stimulate SV endocytosis dye uptake.
3. Immediately start a digital timer for the pre-determined duration of the high [K^+] depolarizing stimulation period (*e.g.*, 5 min; **Figure 2**).
4. To confirm a healthy larval preparation, note the strong contractions of the musculature for the duration of the high [K^+] depolarization period.
5. When the timer period ends, quickly remove the high [K^+] FM dye solution and replace with Ca^{2+}-free saline to stop SV cycling.
6. Wash in quick succession with the Ca^{2+}-free saline (5x for 1 min) to ensure the high [K^+] FM dye solution is completely removed.
7. Maintain the larval preparation in fresh Ca^{2+}-free saline for immediate imaging with the confocal microscope.

3. Imaging: Confocal Microscopy

1. Use an upright confocal microscope with a 40X water immersion objective to image NMJ dye fluorescence (other microscopes can be used).
2. Image muscle 4 NMJ of abdominal segments 2-4 (other NMJs can be imaged) and collect images using appropriate software (**Table of Materials**).
3. Use a HeNe 633 nm laser to excite HRP:647 (with long-pass filter > 635 nm) and an Argon 488 nm laser to excite FM1-43 (with bandpass filter 530-600 nm).
4. Operationally determine optimal gain and offset for both channels.
   NOTE: These settings will remain constant throughout the rest of the experiment.
5. Take a confocal Z-stack through the entire selected NMJ from the HRP-marked top to bottom of the synaptic terminal.

6. Take careful note of the NMJ imaged (segment, side and muscle) to ensure excess to the exact same NMJ after FM dye unloading.

4. High [K^+] Stimulation: FM Dye Unloading

1. Replace Ca^{2+}-free saline with the high [K^+] saline (without FM1-43 dye) to drive depolarization, SV exocytosis and dye release.
2. Immediately start a digital timer for the pre-determined duration of the high [K^+] stimulation period (*e.g.*, 2 min; **Figure 2**).
3. When the timer period ends, immediately remove the high [K^+] saline and replace with Ca^{2+}-free saline to stop SV cycling.
4. Wash in quick succession with Ca^{2+}-free saline (5x for 1 min) to ensure the high [K^+] saline is completely removed.
5. Maintain the larval preparation in fresh Ca^{2+}-free saline for immediate imaging with the confocal microscope.
6. Be certain to image the FM1-43 dye fluorescence at the same NMJ noted above using the same confocal settings.

5. Option 2: Electrical Stimulation FM Dye Loading

1. Prepare a suction pipette using the microelectrode puller (**Table of Materials**) to obtain the required taper and tip size.
2. Fire-polish the microelectrode tip with a micro-forge until a single motor nerve can be sucked up with a tight fit.
3. Slide suction pipette onto the electrode holder on a micromanipulator and attach to the long flexible plastic tube and a syringe.
4. Set stimulator parameters (*e.g.*, 15 V, 20 Hz frequency, 20 ms duration and time of 5 min (**Figure 2**) or 1 min (**Figure 3**)).
5. Replace the Ca^{2+}-free saline on the larval preparation with above FM1-43 saline (4 µM; 1 mM $CaCl_2$) on the electrophysiology rig.
6. Put the preparation on the microscope stage and raise the stage until the larva and suction pipette are in focus (40X water-immersion objective).
7. Suck up a loop of cut motor nerve innervating the selected hemisegment with negative air pressure generated by the syringe into the suction electrode.
8. Test the suction electrode function with a short burst of stimulation while visually monitoring for the muscle contraction in the selected hemisegment.
9. Stimulate the motor nerve using selected parameters (step 5.4) to drive SV endocytosis and FM1-43 dye uptake (**Figure 2**).
10. Wash in quick succession with Ca^{2+}-free saline (5x for 1 min) to ensure the FM1-43 dye solution is completely removed.
11. Maintain the larval preparation in fresh Ca^{2+}-free saline for immediate imaging using the confocal imaging protocol from above.
12. Take careful note of the NMJ imaged (segment, side and muscle) to ensure access to the exact same NMJ after FM dye unloading.

6. Electrical Stimulation: FM Dye Unloading

1. Replace the Ca^{2+}-free saline with regular saline (without FM1-43 dye)and place the preparation back on the electrophysiology rig stage.
2. Set the stimulator parameters for unloading (*e.g.*, 15 V, 20 Hz frequency, 20 ms duration and time of 2 min (**Figure 2**) or 20 s (**Figure 3**)).
3. Suck the same motor nerve into the same electrode as above, and then stimulate to activate SV exocytosis and FM1-43 dye release.
4. Wash in quick succession with Ca^{2+}-free saline (5x for 1 min) to ensure the external dye is completely removed.
5. Maintain the larval preparation in fresh Ca^{2+}-free saline for immediate imaging with the confocal microscope.
6. Ensure to image the FM1-43 dye fluorescence at the same NMJ noted above using the same confocal settings.

7. Option 3: Channelrhodopsin Stimulation FM Dye Loading

1. Raise ChR2-expressing larvae on food containing the ChR2 co-factor all-trans retinal (dissolved in ethanol; 100 µM final concentration).
2. Place the larval preparation in the plexiglass chamber on a dissection microscope stage equipped with a camera port.
3. Attach a blue LED (470 nm; **Table of Materials**) to a programmable stimulator using a coaxial cable and place the LED into the camera port.
4. Focus the blue LED light beam onto the dissected larval function using the microscope zoom function.
5. Replace the Ca^{2+}-free saline on the larval preparation with above FM1-43 saline (4 µM; 1 mM $CaCl_2$) on the optogenetic stage.
6. Set the LED parameters using the stimulator (*e.g.*, 15 V, 20 Hz frequency, 20 ms duration and time of 5 min (**Figure 2**)).
7. Start the light stimulation and track with a timer for the pre-determined duration of the optogenetic stimulation period (*e.g.*, 5 min; **Figure 2**).
8. When the timer stops, quickly remove the FM dye solution and replace with Ca^{2+}-free saline to stop the SV cycling.
9. Wash in quick succession with the Ca^{2+}-free saline (5x for 1 min) to ensure the FM dye solution is completely removed.
10. Maintain the larval preparation in fresh Ca^{2+}-free saline for immediate imaging with the confocal microscope using imaging protocol from above.
11. Take careful note of the NMJ imaged (segment, side and muscle) to ensure access to the exact same NMJ after FM dye unloading.

8. Channelrhodopsin Stimulation: FM Dye Unloading

1. Replace Ca^{2+}-free saline with regular saline (without FM1-43 dye)on the dissection microscope stage with camera port LED focused on the larva.
2. Set the stimulator parameters for unloading (*e.g.,* 15 V, 20 Hz frequency, 20 ms duration and time of 2 min (**Figure 2**)).
3. Start the light stimulation and track with a timer for the pre-determined duration of the optogenetic stimulation period (*e.g.,* 2 min; **Figure 2**).
4. When the timer period ends, quickly remove the FM dye solution and replace with Ca^{2+}-free saline to stop the SV cycling.
5. Wash in quick succession with Ca^{2+}-free saline (5x for 1 min) to ensure the external dye is completely removed.
6. Maintain the larval preparation in fresh Ca^{2+}-free saline for immediate imaging with the confocal microscope.
7. Ensure to image the FM1-43 dye fluorescence at the same NMJ noted above using the same confocal settings.

9. Fluorescence Quantification

1. Load the image in Image J (NIH open source) and create a maximum intensity projection by clicking Image | Stacks | Z Project.
2. Using the anti-HRP:647 channel, go to Image | Adjust | Threshold and slide the top tool bar until just the NMJ is highlighted.
3. Using the wand tool, click on the NMJ. If the NMJ is discontinuous, hold the Shift button and select all parts.
4. Change the image to the FM1-43 dye channel and go to Analyze | Measure to obtain the fluorescence measurement.
5. Repeat steps 9.1-9.4 for the "unloaded" image from the same NMJ (identified segment, side and muscle).
6. To obtain the percentage of dye that was unloaded, take the ratio of the unloaded/loaded fluorescence intensities.
   NOTE: This procedure can be modified to analyze fluorescence on a bouton-per-bouton basis using either the "oval" or "freehand" selection tools. Background fluorescence can be subtracted by sampling the muscle fluorescence. Agents can also be added to reduce this background.

Representative Results

Figure 1 shows the work-flow for the activity-dependent FM dye imaging protocol. The experiment always begins with the same larval glue dissection, regardless of the stimulation method subsequently used. **Figure 1a** is a schematic of a dissected larva, showing the ventral nerve cord (VNC), radiating nerves and repeated hemisegmental muscle pattern. The VNC is removed and the preparation bathed in a 4 µM solution of FM1-43 (**Figure 1b**, pink). The preparation is then stimulated in the presence of FM dye using one of the three possible options to load the dye via activity-dependent SV endocytosis (**Figure 1cI-III**). Next, FM dye cycling is arrested using Ca^{2+}-free saline and a specific NMJ terminal that has been loaded with FM dye is imaged using a confocal microscope ("loaded image"; **Figure 1d**). In this case, the muscle 4 NMJ is selected with the schematic showing placement of the nerve, NMJ terminal branching and FM loaded synaptic boutons. The synaptic preparation is stimulated for a second time using the same method selected above, but in the absence of FM dye to drive SV exocytosis and FM1-43 release (**Figure 1e**). The same identified NMJ (muscle 4 NMJ in this example) is then re-imaged using the HRP:647 synaptic label and residual FM1-43 vesicle signal ("unloaded image"; **Figure 1f**). The experimenter determines the strength and duration of loading and unloading phases to optimize the measurements for a specific assay or mutant condition. Fluorescence intensity is quantified after loading and unloading (**Figure 1d, 1f**), to obtain the measurements of synaptic dye endocytosis, exocytosis and the percentage of loaded FM dye released. Analyses can be done for the entire NMJ or single boutons.

FM dye cycling can be stimulated in three ways: 1) high $[K^+]$ saline depolarization of the entire preparation, 2) suction electrode stimulation of the motor nerve, or 3) light driven activation of targeted channelrhodopsin (ChR2; **Figure 2**). For a direct side-by-side comparison of all three methods, we stimulated with each approach for 5 min in the presence of FM1-43 (loading) and then for 2 min in the absence of FM1-43 (unloading), and imaged HRP-labeled NMJs using identical confocal settings (**Figure 2**). The high $[K^+]$ saline depolarization method follows the widely-used FM1-43 protocol for the *Drosophila* larval NMJ[23], except we use glue instead of pins for the larval dissection. The glue avoids the interference with the microscope objectives and enables more precise determination of body wall tension, but does require a moderate learning curve. All three methods produce strong and consistent fluorescent signals throughout the NMJ synaptic bouton arbor and within individual synaptic boutons (insets). The high $[K^+]$ saline depolarization method causes all NMJs to be FM-loaded throughout the larva as it depolarizes every neuron in the animal (**Figure 2A**, middle). The nerve suction electrode electrical stimulation method drives only in a single hemisegment of the larvae for which the corresponding innervating motor nerve has been stimulated (**Figure 2B**, middle). Unstimulated segments in the same animal are distinguishable using the HRP label but contain no observable fluorescent dye loading, and serve as excellent internal controls. The optogenetic ChR2 method produces targeted depolarization dependent on the transgenic Gal4 driver employed (**Figure 2C**). Here, the driver was a vesicular glutamate transporter (vglut) Gal4, so all glutamatergic neurons are depolarized with blue light stimulation, including all of the glutamatergic motor neurons. As a result, all NMJs are loaded with FM1-43 dye in this example (**Figure 2C**, middle). Cell-specific drivers can be used to label specific NMJs and leave others unlabeled for an internal control.

FM dye unloading was achieved via the same method that was used to load dye. In the first method, the larval preparation was simply bathed in high $[K^+]$ saline in the absence of FM1-43 to depolarize cells, drive SV exocytosis, and unload the synaptic terminals (**Figure 2A**, right). We typically select a shorter unloading period (2 min), so unloading is partial and terminals remain visible in the FM channel. Suction electrode electrical stimulation unloading is considerably more challenging, because it involves returning to the same hemisegment, identifying the same nerve, and re-stimulating that nerve in the absence of FM1-43 to drive dye unloading (**Figure 2B**, right). Note that the dye unloading was again partial. The ChR2 unloading entails a second period of blue LED illumination of the larval preparation in the absence of FM1-43 to activate the channels, depolarize the motor neurons and stimulate SV exocytosis dye release (**Figure 2C**, right). With this timescale of unloading (2 min), each of these depolarization methods unloaded only a percentage of the loaded FM1-43 dye, with the high $[K^+]$ strongest and ChR2 weakest in driving dye release (**Figure 2**). We measured the LED light intensity used (140 µW/mm^2), which was in the published range (20-1000 µW/mm^2)[24,25,26]. ChR2 is maximally activated by ~1 mW illumination from 50-200 mW light sources, with ChR2 effectiveness also dependent on the ATR concentration fed to larva[27,28]. Thus, ChR2 stimulation strength can be manipulated. Moreover, the relationship may not remain true with other stimulation strengths, timescales or genotypes. If the experimenter is working with a mutant that has diminished SV endocytosis or unusually fast exocytosis, the stimulation parameters may need to be altered to maintain an observable signal after unloading. The anti-HRP label allows one to identify the NMJ even in the complete absence of the FM signal, but this is not ideal for quantification. In principle, the unloading stimulation could also be of a different type from the loading stimulation.

We recently studied the loss of the secreted synaptic deacylase Notum effects on the SV cycle using electrical stimulation[4]. Here, we extend this analysis to compare 1) high $[K^+]$ depolarization and 2) suction electrode motor nerve stimulation methods (**Figure 3**). We find that both methods give a similar result, showing reduced FM1-43 dye loading in a *Notum* null mutant; however, the degree of the phenotype is distinct between the two methods. After the depolarization with high $[K^+]$ saline for five min, there is a large decrease in loaded fluorescence intensity between genetic background control (w^{1118}) with high levels and *Notum* null mutants ($Notum^{KO}$) with low levels (**Figure 3A**, top). In quantified measurements, normalized FM fluorescence intensity within HRP-outlined NMJ terminals is significantly reduced in the absence of Notum (w^{1118} 1.0 ± 0.05 vs. $Notum^{KO}$ 0.57 ± 0.07; n≥13, p<0.0001; **Figure 3B**). After electrical stimulation at 20 Hz for 1 min, we find an insignificant decrease in loaded FM1-43 intensity between controls and *Notum* nulls when quantifying whole NMJ fluorescence (w^{1118} 1.0 ± 0.05 vs. $Notum^{KO}$ 0.86 ± 0.06; n = 8, p = 0.10; **Figure 3A**, B). When measuring dye incorporation on a bouton-per-bouton basis, we find a significant decrease in dye

loaded with both of the methods. In quantified measurements after stimulation with high [K^+] saline, normalized FM fluorescence intensity per bouton is significantly decreased (w^{1118} 1.0 ± 0.02 vs. $Notum^{KO}$ 0.52 ± 0.02; n≥241, p<0.0001; **Figure 3C**). After electrical stimulation, normalized fluorescence intensity per bouton is also significantly decreased, albeit to a lower degree (w^{1118} 1.0 ± 0.02 vs. $Notum^{KO}$ 0.83 ± 0.02; n≥127, p<0.0001; **Figure 3C**).

The result differences between the two stimulation paradigms could be due to a number of factors. First, the stimulation strength is presumed to be greater with high [K^+] compared to electrical motor nerve stimulation. Electrophysiology recordings cannot be done in the presence of the high [K^+] saline, but the larval neuromusculature is clearly being robustly stimulated, as muscle contractions are strong and continual throughout the 5 min bathing period. However, we do not know the strength or frequency of the stimulation. In contrast, the electrical stimulation is much more controlled with the user choosing the exact voltage strength and frequency of stimulation. Second, the stimulation duration was longer with high [K^+] compared to electrical nerve stimulation (**Figure 3**). We chose 1 min of 20 Hz electrical stimulation after repeated trials. After 1 min of dye loading, there was a strong and reliable FM1-43 signal, so we chose that paradigm for our study[4], although 5 min of stimulation gave an even stronger fluorescent signal (**Figure 2**). Thus, the length of the stimulation paradigm is likely contributing to the magnitude variability in FM1-43 loading between high [K^+] and electrical stimulation (**Figure 3B, C**). Although the high [K^+] method showed a more robust phenotype for *Notum* mutants, we still used the electrical method because of the greater control[4]. There are many parameters to control such as strength, frequency and duration of stimulation, and those settings must be decided based on the mutant and the question. For example, the stimulation method choice may depend on the SV pool interrogated[7] and the activity-dependent mechanism investigated[10].

After FM1-43 loading into the NMJ terminal, one can employ fluorescence dye photoconversion to produce the electron-dense signal for electron microscopy (**Figure 4**). In this method, the dye-loaded preparation is exposed to intense fluorescent light in the presence of diaminobenzidine (DAB), with the reactive oxygen species from the FM dye oxidizing the DAB to create a dark precipitate (**Figure 4A**)[11]. Please see the JoVE article on photoconversion of styryl dyes for complete details[12]. The benefit of this method is that SVs are clearly revealed at an ultrastructural level, although the SV cycle is of course arrested with static electron microscope imaging. In the absence of stimulation, synaptic boutons at the *Drosophila* NMJ are densely loaded with vesicles (~40 nm in diameter; **Figure 4B**), with the rare occurrence of enlarged organelles (**>**100 nm in diameter) presumed to be cycling endosomes. High [K^+] saline depolarizing stimulation strongly changes this profile, with a partial depletion of the SV population and the rapid accumulation of numerous enlarged organelles (**>**100 nm in diameter) thought to derive from bulk endocytosis of the plasma membrane (**Figure 4C**, left). Although similar compartments exist in unstimulated controls, the high density of these organelles after high [K^+] saline depolarization raises the concern that this may be a non-physiological response. Suction electrode electrical stimulation of the motor nerve is relatively more efficient in depleting the SV population and does not produce more of the enlarged endosomal vesicles (**Figure 4D**, left). This suggests that the bulk endocytosis driven by high [K^+] depolarization helps maintain the SV population during more intense demand.

FM1-43 photoconversion can be accomplished using either high [K^+] saline depolarization or suction electrode electrical stimulation of the motor nerve, to compare synaptic ultrastructure relative to a resting bouton (**Figure 4**). With high [K^+] depolarizing stimulation, both individual SVs and enlarged vesicles (**>**100 nm in diameter) can be labeled with the electron-dense DAB precipitate following light-driven photoconversion (**Figure 4C**, right). For unknown reasons, the enlarged vesicle membrane is typically less densely labeled than the smaller SV membrane. Moreover, SVs often appear filled with the DAB precipitate, rather than just the membrane, but this does make them much easier to distinguish from the unlabeled vesicles. With suction electrode stimulation of the motor nerve, the cycling SV population can also be marked relative to unlabeled SVs (**Figure 4D**, right). With electrical stimulation, enlarged vesicles (**>**100 nm in diameter) are not detectably formed in boutons and, consistently, the membranes of the presumed endosomes are not labeled by FM1-43 photoconversion. As above, cycling SVs are typically filled with the DAB precipitate in a somewhat all-or-none fashion, and therefore more easily distinguishable from SVs that have not been formed during the stimulation (**Figure 4D**, right). We have not yet attempted photoconversion following ChR2 stimulation. With different time courses of stimulation, FM1-43 dye photoconversion allows one to determine where SVs are formed, how SVs are trafficked, and the timing of movement between different spatial pools within the synaptic bouton. The comparison of high [K^+] and nerve stimulation allows the dissection of bulk and single SV endocytosis mechanisms.

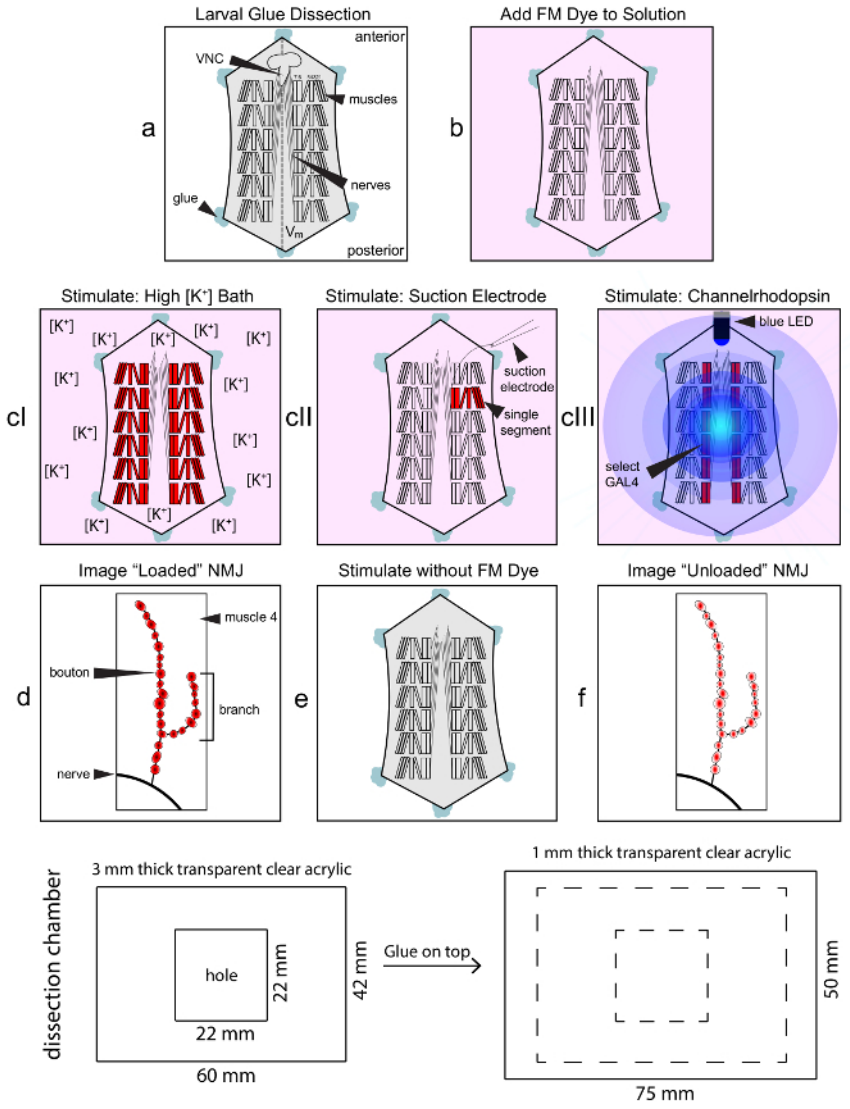

Figure 1: Flowchart of FM1-43 dye loading protocol at the *Drosophila* NMJ. The larval glue dissection produces a flattened neuromusculature preparation, with the ventral nerve cord (VNC) projecting segmental nerves from the ventral midline (Vm) to the hemisegmentally repeated body wall muscle arrays (step a). The VNC is cut free, and the entire larval dissection is then incubated in the pink FM1-43 solution (4 µM) in preparation for stimulation (step b). FM1-43 is then loaded with a selected stimulation paradigm (step 3); with the options of high [K^+] depolarization of the entire larva (cI), suction electrode stimulation of a single motor nerve (cII), or light-driven activation of highly targeted channelrhodopsin (cIII). FM1-43 incorporation is arrested using Ca^{2+}-free saline and the dye-loaded NMJ imaged (step d). A second stimulation is then done without FM1-43 in the bath to drive dye synaptic vesicle exocytosis (step e). The same NMJ is then re-imaged to assay the unloaded synaptic terminal (step f). Fluorescent intensity is measured from both loaded and unloaded NMJs to quantify SV endocytosis and SV exocytosis levels. The bottom panel shows the construction parameters and dimensions for the transparent acrylic chamber used for these studies. Please click here to view a larger version of this figure.

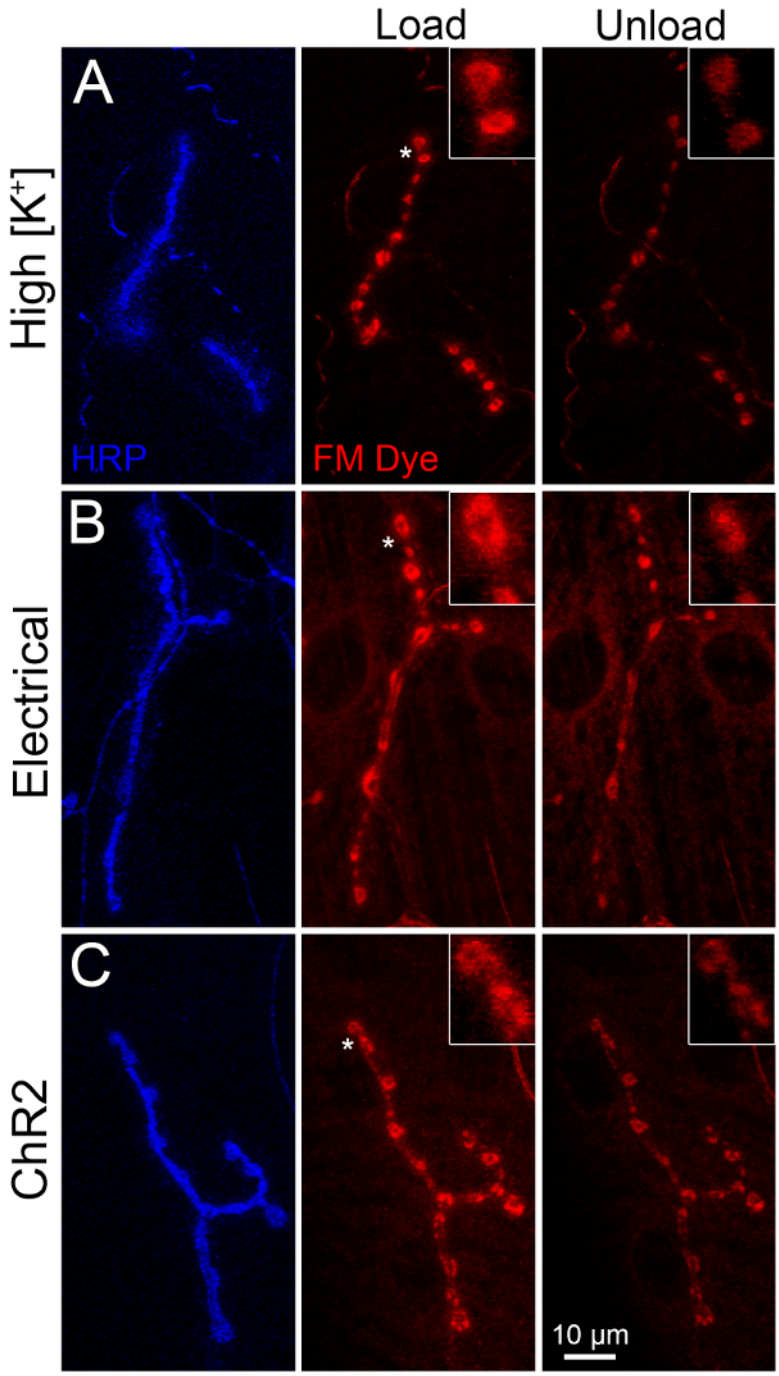

Figure 2: FM dye loading and unloading comparison of all stimulation methods. Comparison of FM1-43 dye loading and unloading in the wandering third instar NMJ with 1) high [K^+] depolarization of the entire larval preparation (top), 2) suction electrode electrical stimulation of the motor nerve (middle) and 3) light-driven activation of the targeted channelrhodopsin (ChR2) only in motor neurons (bottom). (**A**) The larval NMJ labeled with the anti-HRP:647 presynaptic membrane marker (blue, left), loaded with FM1-43 via high [K^+] depolarization for 5 min (middle) and then unloaded via high [K^+] depolarization for 2 min. (**B**) Comparison with suction electrode electrical nerve stimulation with the same stimuli periods for both FM1-43 dye loading and unloading. (**C**) Targeted *vglut*-Gal4**>**UAS-ChR2-H134R expression in motor neurons activated with blue (470 nm) light for the same stimuli periods of FM1-43 dye loading and unloading. Asterisks refer to insets displaying higher magnification boutons. The scale bar is 10 µm, with inset synaptic boutons enlarged 3.5X from main panels. Please click here to view a larger version of this figure.

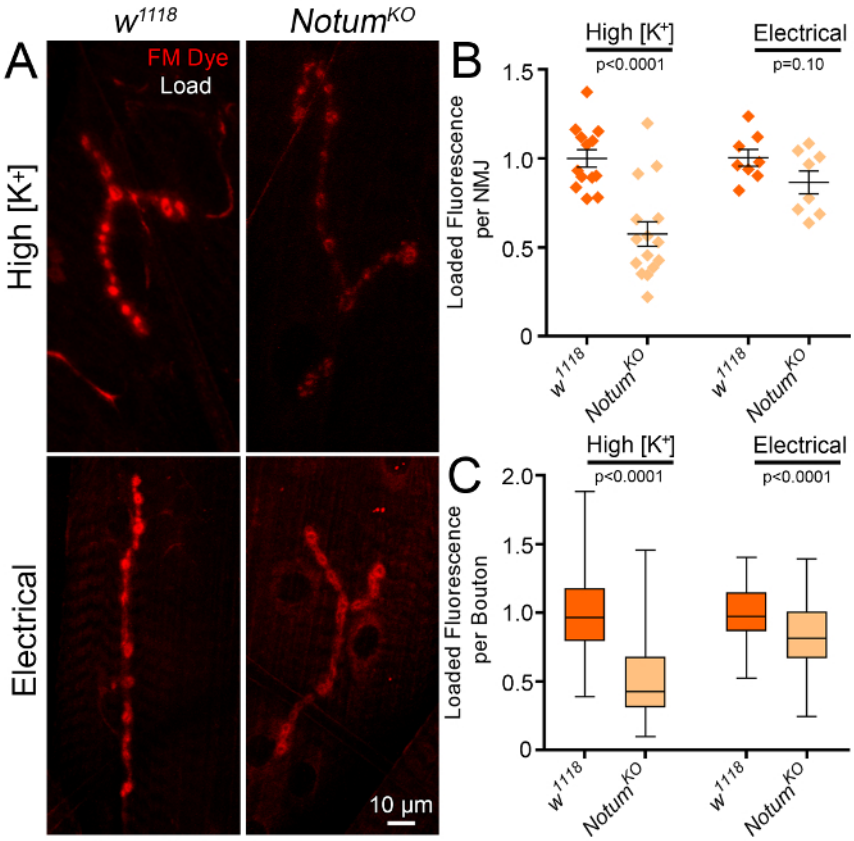

Figure 3: *Notum* null mutants show reduced FM dye loading in synaptic boutons. FM1-43 loaded into synaptic terminals of the wandering third instar NMJ comparing the genetic control (w^{1118}) to *Notum* null mutants ($Notum^{KO}$). (**A**) NMJ boutons labeled with high [K^+] depolarization of entire larval preparation (top) or suction electrode stimulation of one motor nerve (bottom) in w^{1118} (left) and $Notum^{KO}$ (right). (**B**) Quantified loaded FM1-43 fluorescence per NMJ as a scatter plot comparing the high [K^+] depolarization and suction electrode stimulation in w^{1118} controls vs. $Notum^{KO}$ mutants. (**C**) Quantified loaded fluorescence on a bouton-per-bouton basis as a box-and-whisker plot comparing high [K^+] depolarization and suction electrode stimulation in w^{1118} controls vs. $Notum^{KO}$. Student's two-tailed t-tests were performed for each comparison with p-values displayed on the graphs. Bars show mean ± SEM made with Prism (Version 7.0 for Windows). The electrical stimulation data has been adapted with permission from Kopke *et al*., Development 144(19):3499-510, 2017. Please click here to view a larger version of this figure.

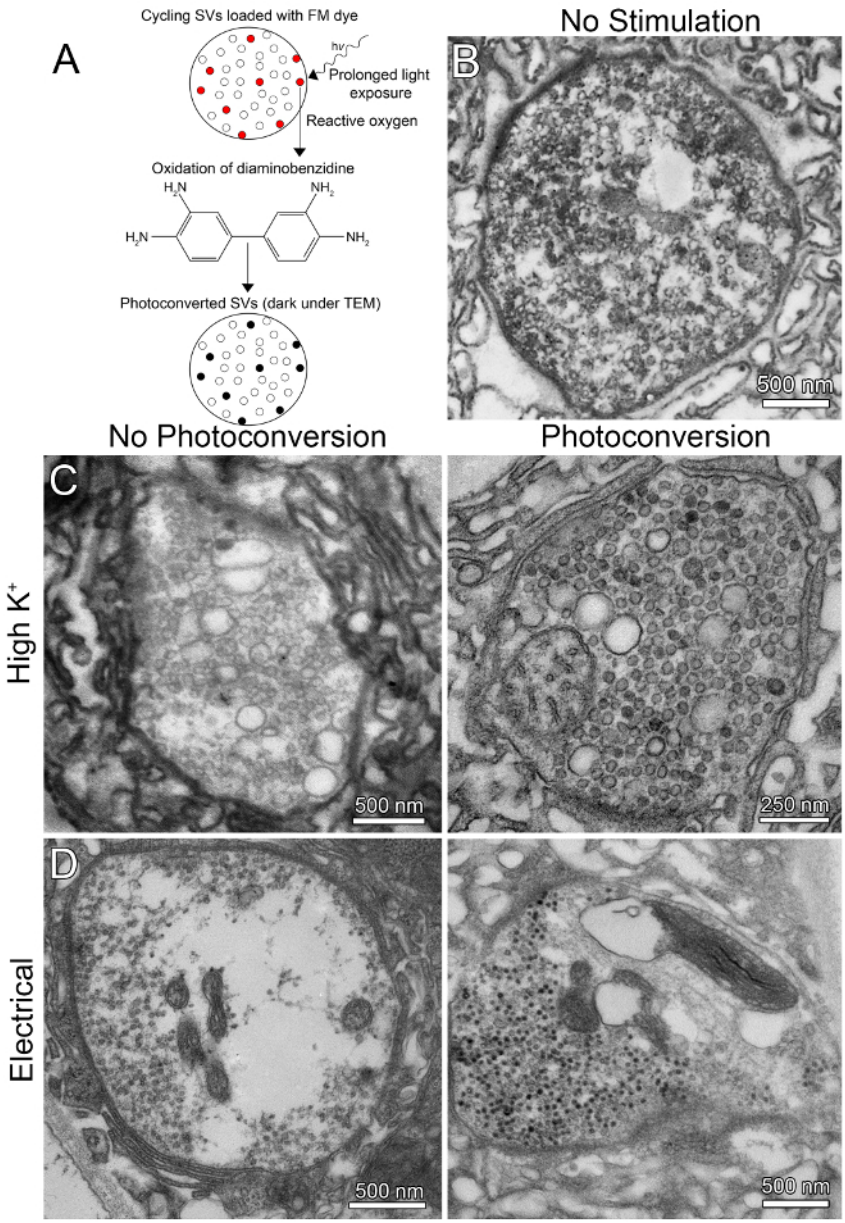

Figure 4: Synaptic ultrastructure with FM dye photoconversion to mark vesicles. Fluorescent FM1-43 can be photoconverted to an oxidized diaminobenzidine (DAB) electron-dense precipitate for visualization via transmission electron microscopy (TEM). (**A**) A schematic diagram of the photoconversion method to label the *Drosophila* NMJ following activity-dependent FM1-43 dye loading. (**B**) Representative TEM image of a wildtype synaptic bouton at rest (unstimulated). Note dense population of uniform-sized SVs. (**C**) Synaptic boutons that have been stimulated with high [K^+] saline depolarization for 5 min, without photoconversion (left) or with FM1-43 photoconversion (right). Note the presence of bulk endosomal structures, labeled and unlabeled. (**D**) Synaptic boutons that have been electrically stimulated with a nerve suction electrode at 20 Hz for 5 min with no photoconversion (left) or with FM1-43 photoconversion (right). Note that the dye-loaded vesicles appear much darker than adjacent unloaded vesicles. Please click here to view a larger version of this figure.

Discussion

High [K^+] saline depolarizing stimulation is by far the easiest of the three options for activity-dependent FM dye cycling, but likely the least physiological[29]. This simple method depolarizes every accessible cell in the entire animal, and so does not allow directed studies. It may be possible to locally apply high [K^+] saline with a micropipette, but this will still depolarize pre/postsynaptic cells and likely synapse-associated glia[1]. Another major concern is that high [K^+] depolarization drives rapid formation of bulk endosomes that are only rarely seen in unstimulated boutons. However, bulk endosome formation is an active mechanism blocked by mutations[29], indicating a real physiological process. Thus, FM1-43 imaging with high [K^+] depolarization can be used to selectively study bulk endocytosis at synapses. Suction electrode electrical stimulation of the motor nerve is a much more controlled method. It has the advantage that only a single axon bundle is stimulated, and only the presynaptic termini is directly depolarized (of course, the muscle fiber is then depolarized by transmitter action). It therefore provides a great internal control of NMJs in the same animal that are not stimulated. This method allows one to tightly control the stimulation parameters, unlike

the high [K^+] stimulation method, enabling direct comparison with electrophysiology recordings[4]. However, this technique requires specialized equipment and a fairly high level of technical skill, and is therefore less accessible. Light-driven activation of targeted channelrhodopsin (ChR2) has the advantage of targeting select neurons[30]. This method requires no familiarity with electrophysiology methods, and can be done with very cheap equipment in any lab, but this approach does require basic familiarity with *Drosophila* genetics.

The choice of stimulation parameters is critically important for testing SV cycle dynamics queried within a range of genetic conditions with highly variable phenotypes[1]. For all methods, the external [Ca^{2+}] used is a key parameter controlling the driving force of SV cycling. With the high [K^+] stimulation method, an important choice is [K^+] used, which determines the degree of depolarization strength. Measurements of *Drosophila* haemolymph indicate a [K^+] of 5 mM, and 90 mM is typically the concentration most often selected for activity stimulation[3,7,15,17,31]. However, a [K^+] range from 30-90 mM has been employed to vary the stimulation strength[5,16,32]. Another critical parameter decision is the length of the high [K^+] stimulation for both FM1-43 loading and unloading. The period for loading determines whether the entire cycling SV population is effectively loaded, or only a subset of active vesicles[7]. The period for unloading similarly dictates the percentage of SVs undergoing exocytosis in the stimulation period, which can either reveal or obscure mutant phenotypes dependent on rate changes in the SV cycling frequency[2]. With suction electrode electrical motor nerve stimulation, parameter choices include also stimulation voltage, frequency, duration and pulse interval. Temporally patterned activity is a key determinant of SV cycling dynamics[7], and different stimulation patterns can selectively mobilize distinct SV pools. With targeted light-driven ChR2 activation, the choices include all of the above (with light intensity variables) and additional transgenic options discussed in the next section. With these parameter, choices comes more experimental control, but also increased technical complexity.

Channelrhodopsin-2 (ChR2) is a light-gated membrane channel permeable to mono- and divalent cations[33]. If ChR2 stimulation is selected, there are many choices to be made including the Gal4 driver, UAS-ChR2 construct and light source variables for channel activation. Gal4 drivers range from ubiquitous to highly specific. For example, ubiquitous UH1-Gal4 (*daughterless*) would express ChR2 in every cell, whereas CcapR-Gal4 (Janelia) drives ChR2 in the muscle 6/7 NMJ but not the muscle 4 NMJ[31,34]. This selectivity can be used as a powerful internal control. There are likewise many UAS-ChR2 variants, including ChR2-H134R (used here; the mutated residue causes increased photocurrents)[35], VChR1, ChIEF and many more[36]. Each of these channel variants has distinct properties of light gating, conductance, ion selectivity, kinetics and desensitization. Note some constructs contain a fluorescent tag that could interfere with FM imaging. For example, the UAS-ChR2-H134R used here is tagged with mCherry (ex: 587 nm, em: 610 nm), but does not produce detectible emission with the FM1-43 (ex: 479 nm, em: 598 nm) imaging filters. Technical parameter choices include the light source, wavelength and intensity for channel activation. An option used here is a cheap blue-emitting LED, with stimulation visually confirmed by assaying muscle contractions. We were also successful in activating ChR2 using epifluorescence, although a scanning confocal laser was not sufficient. Epifluorescence could be used in targeted stimulation (specific segments instead of the whole animal), but stimulation parameters are difficult to control, whereas the LED connected up to a simple stimulator easily alters both the duration and frequency of light pulses. Focusing the LED light through the dissection microscope camera port allows more controlled, intense light stimulation.

It is up to the experimenter to decide whether or not to leave the ventral nerve cord/brain intact during the stimulation paradigm. We chose to remove the entire central nervous system for the comparison of the three methods used here, but sometimes the upstream wiring is left intact[15]. A complication is that endogenous neural activity occurs whenever the nervous system is left whole. The degree of this activity is highly variable from animal to animal, dependent in large degree on the dissection expertise of the experimenter. This variable activity can contribute to the amount of FM1-43 dye that is loaded and unloaded, which is therefore not solely due to the exogenous stimulation employed[15]. A related technical complication is that intact dissected larvae contract the musculature in fictive movement, and this displacement greatly interferes with NMJ imaging. This movement is alleviated if the central nervous system is removed, and also through the application of Ca^{2+}-free saline during imaging[4]. These approaches used here are sufficient to enable excellent FM1-43 dye imaging in the NMJ preparation. However, some experimenters choose to add drugs to inhibit muscle contraction (*e.g.,* ryanodine, philanthotoxin-433), or use action potential blockers (*e.g.,* tetrodotoxin)[37,38]. A range of drugs can be used to selectively manipulate the SV cycle, in order to highlight certain steps, or accentuate mutant phenotypes to examine neurotransmission mechanisms. For example, some experimenters have employed Veratridine (activates voltage-gated Na^+ channels[39]) to increase SV loading in the reserve pool, Cyclosporin A (inhibits Calcineurin activity[40]) to enhance SV endocytosis, and Forskolin (activates adenylyl cyclase[41], which enhances synaptic transmission[42]) to increase the exo/endo cycling pool[7,43,44]. Such pharmacological manipulations can provide additional insights. Lastly, FM1-43 background can occur to varying degrees based on quality of dissection, washing effectiveness and stimulation protocol. Some add a sulfobutylated derivative of β-cyclodextrin Advasep-7[45], or the aqueous fluorophore sulforhodamine[46], to quench nonspecific fluorescence and improve signal-to-background ratio.

There are numerous techniques that can accompany FM fluorescent imaging to further understanding of the SV cycle (*e.g.,* electrophysiology, synaptopHluorin, electron microscopy). An example shown here is FM fluorescence photoconversion that is used to investigate the SV cycle in ultrastructural detail. SVs are organized into several pools that are spatially and functionally distinct[2]. The readily releasable pool (RRP) contains vesicles immediately released upon acute stimulation. A larger recycling pool maintains SV release under conditions of moderate activity. An internal reserve pool (RP) is only recruited with strong (seemingly near non-physiological) stimulation[2]. The SV pools that are activated depend on the type of stimulation used[47], and reports from the *Drosophila* NMJ using FM photoconversion have revealed key insights into spatial and functional properties of these different SV pools[48]. FM photoconversion can be used to study SV pools activated under different stimulation paradigms, and query questions such as the long-debated trafficking interaction between endosomes and SVs[49]. If the experimenter is interested in FM imaging in combination with other activity-dependent changes at the synapse, there is a reportedly fixable analog of the FM1-43 dye (FM1-43FX). This probe should allow one to fix the *Drosophila* NMJ after activity-dependent dye loading, and then follow up with antibody labeling to test for correlations between bouton activity level (FM dye fluorescence) and activity-dependent expression of a protein of interest. In the future, it will be extremely rewarding to explore additional methods that could enable the combination of FM dye imaging with other imaging approaches at the beautiful *Drosophila* NMJ model synapse.

Disclosures

The authors declare no competing interests.

Acknowledgements

We thank Broadie Lab members for contributions to this article. This work was supported by NIH R01s MH096832 and MH084989 to K.B., and NIH predoctoral fellowship F31 MH111144 to D.L.K.

References

1. Menon, K.P., Carrillo, R.A., Zinn, K. Development and plasticity of the *Drosophila* larval neuromuscular junction. *Wiley Interdiscip Rev Dev Biol.* **2** (5), 647-670 (2013).
2. Rizzoli, S.O., Betz, W.J. Synaptic vesicle pools. *Nat Rev Neurosci.* **6** (1), 57-69 (2005).
3. Long, A.A. *et al.* Presynaptic calcium channel localization and calcium-dependent synaptic vesicle exocytosis regulated by the Fuseless protein. *J Neurosci.* **28** (14), 3668-82 (2008).
4. Kopke, D.L., Lima, S.C., Alexandre, C., Broadie, K. Notum coordinates synapse development via extracellular regulation of Wingless trans-synaptic signaling. *Development.* **144** (19), 3499-3510 (2017).
5. Betz, W.J., Mao, F., Bewick, G.S. Activity-dependent fluorescent staining and destaining of living vertebrate motor nerve terminals. *J Neurosci.* **12** (2), 363-75, at <http://www.ncbi.nlm.nih.gov/pubmed/1371312 > (1992).
6. Richards, D.A., Bai, J., Chapman, E.R. Two modes of exocytosis at hippocampal synapses revealed by rate of FM1-43 efflux from individual vesicles. *J Cell Biol.* **168** (6), 929-39 (2005).
7. Verstreken, P., Ohyama, T., Bellen, H.J. FM 1-43 labeling of synaptic vesicle pools at the *drosophila* neuromuscular junction. *Methods Mol Biol.* **440**, 349-369 (2008).
8. Dickman, D.K., Horne, J.A., Meinertzhagen, I.A., Schwarz, T.L. A Slowed Classical Pathway Rather Than Kiss-and-Run Mediates Endocytosis at Synapses Lacking Synaptojanin and Endophilin. *Cell.* **123** (3), 521-533 (2005).
9. Verstreken, P. *et al.* Endophilin Mutations Block Clathrin-Mediated Endocytosis but Not Neurotransmitter Release. *Cell.* **109** (1), 101-112 (2002).
10. Iwabuchi, S., Kakazu, Y., Koh, J.-Y., Goodman, K.M., Harata, N.C. Examination of synaptic vesicle recycling using FM dyes during evoked, spontaneous, and miniature synaptic activities. *J Vis Exp.* (85) (2014).
11. Sandell, J.H., Masland, R.H. Photoconversion of some fluorescent markers to a diaminobenzidine product. *J Histochem Cytochem.* **36** (5), 555-9, at <http://www.ncbi.nlm.nih.gov/pubmed/3356898 > (1988).
12. Opazo, F., Rizzoli, S.O. Studying Synaptic Vesicle Pools using Photoconversion of Styryl Dyes. *J Vis Exp.* (36), e1790-e1790 (2010).
13. Sabeva, N.S., Bykhovskaia, M. FM1-43 Photoconversion and Electron Microscopy Analysis at the *Drosophila* Neuromuscular Junction. *Bio-protocol.* **7** (17) (2017).
14. Sabeva, N., Cho, R.W., Vasin, A., Gonzalez, A., Littleton, J.T., Bykhovskaia, M. Complexin Mutants Reveal Partial Segregation between Recycling Pathways That Drive Evoked and Spontaneous Neurotransmission. *J Neurosci.* **37** (2), 383-396 (2017).
15. Ryan, T.A., Reuter, H., Wendland, B., Schweizer, F.E., Tsien, R.W., Smith, S.J. The kinetics of synaptic vesicle recycling measured at single presynaptic boutons. *Neuron.* **11** (4), 713-724 (1993).
16. Ramaswami, M., Krishnan, K.S., Kelly, R.B. Intermediates in synaptic vesicle recycling revealed by optical imaging of *Drosophila* neuromuscular junctions. *Neuron.* **13** (2), 363-375 (1994).
17. Trotta, N., Rodesch, C.K., Fergestad, T., Broadie, K. Cellular bases of activity-dependent paralysis in *Drosophila* stress-sensitive mutants. *J Neurobiol.* **60** (3), 328-347 (2004).
18. Long, A.A. *et al.* The nonsense-mediated decay pathway maintains synapse architecture and synaptic vesicle cycle efficacy. *J Cell Sci.* **123** (Pt 19), 3303-15 (2010).
19. Parkinson, W., Dear, M.L., Rushton, E., Broadie, K. N-glycosylation requirements in neuromuscular synaptogenesis. *Development.* **140** (24), 4970-81 (2013).
20. Brand, A.H., Perrimon, N. Targeted gene expression as a means of altering cell fates and generating dominant phenotypes. *Development.* **118** (2), 401 LP-415, at <http://dev.biologists.org/content/118/2/401.abstract > (1993).
21. Jan, L.Y., Jan, Y.N. Antibodies to horseradish peroxidase as specific neuronal markers in *Drosophila* and in grasshopper embryos. *Proc Natl Acad Sci.* **79** (8) (1982).
22. Paschinger, K., Rendić, D., Wilson, I.B.H. Revealing the anti-HRP epitope in *Drosophila* and Caenorhabditis. *Glycoconj J.* **26** (3), 385-395 (2009).
23. Ramachandran, P., Budnik, V. Fm1-43 labeling of *Drosophila* larval neuromuscular junctions. *Cold Spring Harb Protoc.* **2010** (8) (2010).
24. Yawo, H., Kandori, H., Koizumi, A. *Optogenetics: light-sensing proteins and their applications.* (2015).
25. Pulver, S.R., Pashkovski, S.L., Hornstein, N.J., Garrity, P.A., Griffith, L.C. Temporal dynamics of neuronal activation by Channelrhodopsin-2 and TRPA1 determine behavioral output in *Drosophila* larvae. *J Neurophysiol.* **101** (6), 3075-88 (2009).
26. Hornstein, N.J., Pulver, S.R., Griffith, L.C. Channelrhodopsin2 Mediated Stimulation of Synaptic Potentials at *Drosophila* Neuromuscular Junctions. *J Vis Exp.* (25), e1133-e1133 (2009).
27. Britt, J.P., McDevitt, R.A., Bonci, A. Use of channelrhodopsin for activation of CNS neurons. *Curr Protoc Neurosci.* **Chapter 2**, Unit 2.16 (2012).
28. Lin, J.Y. A user's guide to channelrhodopsin variants: features, limitations and future developments. *Exp Physiol.* **96** (1), 19-25 (2011).
29. Vijayakrishnan, N., Woodruff, E.A., Broadie, K. Rolling blackout is required for bulk endocytosis in non-neuronal cells and neuronal synapses. *J Cell Sci.* **122** (Pt 1), 114-25 (2009).
30. Honjo, K., Hwang, R.Y., Tracey, W.D. Optogenetic manipulation of neural circuits and behavior in *Drosophila* larvae. *Nat Protoc.* **7** (8), 1470-1478 (2012).
31. Dear, M.L., Shilts, J., Broadie, K. Neuronal activity drives FMRP- and HSPG-dependent matrix metalloproteinase function required for rapid synaptogenesis. *Sci Signal.* **10** (504), eaan3181 (2017).
32. Baldwin, M.L., Rostas, J.A.P., Sim, A.T.R. Two modes of exocytosis from synaptosomes are differentially regulated by protein phosphatase types 2A and 2B. *J Neurochem.* **85** (5), 1190-1199 (2003).

33. Nagel, G. *et al.* Channelrhodopsin-2, a directly light-gated cation-selective membrane channel. *Proc Natl Acad Sci U S A.* **100** (24), 13940-5 (2003).
34. Pfeiffer, B.D. *et al.* Tools for neuroanatomy and neurogenetics in *Drosophila. Proc Natl Acad Sci U S A.* **105** (28), 9715-20 (2008).
35. Nagel, G., Brauner, M., Liewald, J.F., Adeishvili, N., Bamberg, E., Gottschalk, A. Light Activation of Channelrhodopsin-2 in Excitable Cells of Caenorhabditis elegans Triggers Rapid Behavioral Responses. *Curr Biol.* **15** (24), 2279-2284 (2005).
36. Lin, J.Y. A user's guide to channelrhodopsin variants: features, limitations and future developments. *Exp Physiol.* **96** (1), 19-25 (2011).
37. Sullivan, K.M., Scott, K., Zuker, C.S., Rubin, G.M. The ryanodine receptor is essential for larval development in *Drosophila* melanogaster. *Proc Natl Acad Sci U S A.* **97** (11), 5942-7 (2000).
38. Narahashi, T., Moore, J.W., Scott, W.R. Tetrodotoxin Blockage of Sodium Conductance Increase in Lobster Giant Axons. *J Gen Physiol.* **47** (5), 965-74 (1964).
39. Narahashi, T. Chemicals as tools in the study of excitable membranes. *Physiol Rev.* **54** (4), 813-89 (1974).
40. Kuromi, H., Yoshihara, M., Kidokoro, Y. An inhibitory role of calcineurin in endocytosis of synaptic vesicles at nerve terminals of *Drosophila* larvae. *Neurosci Res.* **27** (2), 101-113 (1997).
41. Seamon, K.B., Daly, J.W. Forskolin, cyclic AMP and cellular physiology. *Trends Pharmacol Sci.* **4**, 120-123 (1983).
42. Zhang, D., Kuromi, H., Kidokoro, Y. Synaptic Transmission at the *Drosophila* Neuromuscular Junction: Effects of Metabotropic Glutamate Receptor Activation. *Slow Synaptic Responses Modul.* 260-265 (2000).
43. Kuromi, H., Kidokoro, Y. The optically determined size of exo/endo cycling vesicle pool correlates with the quantal content at the neuromuscular junction of *Drosophila* larvae. *J Neurosci.* **19** (5), 1557-65, at <http://www.ncbi.nlm.nih.gov/pubmed/10024343> (1999).
44. Kuromi, H., Kidokoro, Y. Selective Replenishment of Two Vesicle Pools Depends on the Source of Ca2+ at the *Drosophila* Synapse. *Neuron.* **35** (2), 333-343 (2002).
45. Kay, A.R. *et al.* Imaging Synaptic Activity in Intact Brain and Slices with FM1-43 in C. elegans, Lamprey, and Rat. *Neuron.* **24** (4), 809-817 (1999).
46. Pyle, J.L., Kavalali, E.T., Choi, S., Tsien, R.W. Visualization of Synaptic Activity in Hippocampal Slices with FM1-43 Enabled by Fluorescence Quenching. *Neuron.* **24** (4), 803-808 (1999).
47. Denker, A., Rizzoli, S.O. Synaptic vesicle pools: an update. *Front Synaptic Neurosci.* **2**, 135 (2010).
48. Denker, A., Kröhnert, K., Rizzoli, S.O. Revisiting synaptic vesicle pool localization in the *Drosophila* neuromuscular junction. *J Physiol.* **587** (12), 2919-2926 (2009).
49. Wucherpfennig, T., Wilsch-Bräuninger, M., González-Gaitán, M. Role of *Drosophila* Rab5 during endosomal trafficking at the synapse and evoked neurotransmitter release. *J Cell Biol.* **161** (3), 609-24 (2003).

